

1 The splitting of directed flow for identified light hadrons (K
2 and p) and strange baryons (Ξ and Ω) in Au+Au collisions
3 at STAR *

4 ASHIK IKBAL SHEIKH (FOR THE STAR COLLABORATION)

5 Department of Physics, Kent State University,
6 Kent, OH 44242, USA
7 Email: asheikh2@kent.edu, ashikhep@gmail.com

8 *Received July 29, 2022*

9 The first measurements for rapidity-odd directed flow of Ξ and Ω in
10 Au+Au collisions at $\sqrt{s_{NN}} = 27$ and 200 GeV are reported. The coales-
11 cence sum rule is examined with various combinations of hadrons where all
12 constituent quarks are produced, such as $K^-(\bar{u}s)$, $\bar{p}(\bar{u}\bar{u}\bar{d})$, $\bar{\Lambda}(\bar{u}\bar{d}\bar{s})$, $\phi(s\bar{s})$,
13 $\bar{\Xi}^+(\bar{d}\bar{s}\bar{s})$, $\Omega^-(sss)$, and $\bar{\Omega}^+(\bar{s}\bar{s}\bar{s})$. For such combinations, a systematic vio-
14 lation of the sum rule is observed with increasing difference in the electric
15 charge and the strangeness content of the combinations. Measurements are
16 compared with the calculations of A Multi-Phase Transport (AMPT) model
17 and Parton-Hadron String Dynamics (PHSD) model with electromagnetic
18 (EM) field. The PHSD model with EM field agrees with the measurements
19 within uncertainties.

20 **1. Introduction**

21 Directed flow (v_1) is the first harmonic coefficient in the Fourier expan-
22 sion of the final-state azimuthal distribution relative to the reaction plane.
23 Theoretical calculations [1] based on nuclear transport and hydrodynam-
24 ics indicate that the v_1 is sensitive to the early stages of the high energy
25 heavy-ion collisions.

26 One of the most important features of the early stages of the heavy-ion
27 collisions is the production of an extremely strong magnetic field due to
28 the motion of the charged spectators. The produced magnetic field decays
29 down fast since the charged spectators fly away from the collision zone
30 and this generates an electric current in the plasma due to the Faraday
31 effect. In addition, the plasma has a longitudinal expansion velocity along

* Presented at 29th International Conference on Ultra-relativistic Nucleus-Nucleus Col-
lisions (Quark Matter 2022), Krakow, Poland

32 the beam direction and perpendicular to magnetic field direction, hence the
 33 Lorentz force pushes charged particles and anti-particles of the plasma in
 34 opposite ways which are perpendicular to both the directions of longitudinal
 35 velocity of plasma and the magnetic field. This is analogous to Hall effect.
 36 The charged spectators can also generate an electric current in the plasma
 37 due to Coulomb effect. The v_1 of different produced charged particles is
 38 greatly influenced by the resultant of Faraday, Hall, and Coulomb effects
 39 which eventually leads to the splitting of v_1 [2]. Both STAR and ALICE
 40 experiments measured a non-zero v_1 splitting with pseudo-rapidity between
 41 positively and negatively charged hadrons in Au+Au collisions at $\sqrt{s_{NN}} =$
 42 200 GeV [3] and Pb+Pb collisions at $\sqrt{s_{NN}} = 2.76$ TeV [4], respectively.
 43 However, the interpretation of the measured splitting using charged hadrons
 44 runs into difficulties especially when the effects of electromagnetic fields are
 45 concerned. This is due to the fact that among light hadrons, there are many
 46 (anti-)particles containing u and d quarks, which can be either transported
 47 from beam rapidity [5] or produced in the collisions. Due to the different
 48 number of interactions suffered, the transported u and d have different v_1
 49 than those of the produced quarks [6]. This ensures a pre-existing splitting
 50 due to the transport. This transport driven splitting is a background in
 51 search of the pure electromagnetic-field-driven splitting. We could avoid
 52 the transported quarks in our analysis by selecting particles composed of
 53 produced constituent quarks only (\bar{u} , \bar{d} , s , and \bar{s}). The experimental method
 54 is outlined briefly in Sec. 2.

55 In this contribution, we report the measurements of v_1 of multi-strange
 56 baryons (Ξ and Ω). The v_1 -splitting as a function of electric charge differ-
 57 ence (Δq) and strangeness difference (ΔS) is measured, using K^- , \bar{p} , $\bar{\Lambda}$, ϕ ,
 58 Ξ^+ , Ω^- , and $\bar{\Omega}^+$ from Au+Au collisions at $\sqrt{s_{NN}} = 27$ and 200 GeV.

59 2. Data sets and Analysis strategy

60 STAR detector system is versatile experimental setup for track recon-
 61 struction, vertexing, and particle identification at RHIC. The main sub-
 62 detectors are (i) Time Projection Chamber (TPC) ($|\eta| \leq 1$): used for
 63 charged particle tracking, vertexing, and particle identification; (ii) Time-
 64 Of-Flight (TOF) detector: used for particle identification; (iii) Event-Plane
 65 Detectors (EPDs) ($2.1 < |\eta| < 5.1$) and (iv) Zero-Degree Calorimeter with
 66 Shower-Maximum Detectors (ZDC-SMDs) ($|\eta| > 6.3$): can measure event
 67 planes of the collisions.

68 A high statistics data samples for Au+Au collisions at $\sqrt{s_{NN}} = 27$ and
 69 200 GeV are used in the measurements. We use events with the vertex
 70 position along the beam direction with $|V_z| < 70$ cm, and along the radial
 71 directions, $V_r < 2$ cm at $\sqrt{s_{NN}} = 27$ GeV; and $|V_z| < 30$ cm, $V_r < 2$ cm

72 at $\sqrt{s_{NN}} = 200$ GeV. At the track level, $p_T > 0.2$ GeV/ c , and a distance of
 73 closest approach (DCA) from vertex, $DCA \leq 3$ cm, and at least 15 space
 74 points in the TPC acceptance are selected. For particle identification, we
 75 use $p_T > 0.2$ GeV/ c , momentum < 1.6 GeV/ c and $|n_\sigma| \leq 2$ for charged
 76 pions and kaons; $0.4 < p_T < 5$ GeV/ c , $|n_\sigma| \leq 2$ for p and \bar{p} , where n_σ is
 77 the standard deviation of difference between measured $\langle dE/dx \rangle$ and the-
 78 oretical mean value for each particle type. The Λ , $\bar{\Lambda}$, Ξ^- , $\bar{\Xi}^+$, Ω^- , and
 79 $\bar{\Omega}^+$ are reconstructed using KF-Particle package [7]. The ϕ -mesons are re-
 80 constructed in K^+K^- channel using the invariant mass method with pair
 81 rotation background subtraction. The systematic uncertainties on the mea-
 82 surements are obtained by varying these analysis cuts. We remove the effect
 83 of the statistical fluctuations by employing Barlow’s method [8].

84 The analysis method is based on the quark coalescence mechanism.
 85 Coalescence sum rule states that the directed flow of a hadron is con-
 86 sistent with the sum of the directed flow of its constituent quarks, *i.e.*,
 87 $v_1(\text{hadron}) = \sum_i v_1(q_i)$, where the sum runs over the v_1 of the constituent
 88 quarks, q_i . There are many hadron species composed of constituent u and
 89 d quarks, which might or might not be transported from the incoming nu-
 90 clei. The transported quarks produce background in search of the pos-
 91 sible electromagnetic-field-driven v_1 splitting. Hence, in the analysis we
 92 take particles which contain produced quarks only, namely, $K^-(\bar{u}s)$, $\bar{p}(\bar{u}\bar{u}\bar{d})$,
 93 $\bar{\Lambda}(\bar{u}\bar{d}\bar{s})$, $\phi(s\bar{s})$, $\bar{\Xi}^+(d\bar{s}\bar{s})$, $\Omega^-(sss)$, and $\bar{\Omega}^+(\bar{s}\bar{s}\bar{s})$. All these particles have
 94 different flavour, electric charge (q) and mass (m); and v_1 is sensitive to
 95 quark flavour and mass. Keeping this in mind, we combine the different
 96 particles so that combinations have same or similar mass at the constituent
 97 quark level ($\Delta m \approx 0$), but $\Delta q \neq 0$ and $\Delta S \neq 0$. We found five independent
 98 combinations as shown in Table 1. The difference Δv_1 of such combinations
 99 is called “splitting of v_1 ” [9] and the slope of the Δv_1 vs. rapidity is a
 100 measure of the splitting. We measure the Δv_1 of all the indices in Table 1
 101 to obtain the splitting as a function of Δq , a measure of EM-field-driven
 102 splitting. At the same time, we also measure the the Δv_1 with ΔS of all the
 103 combinations. Although, the change in Δq is also associated with a change
 104 in ΔS in Table 1 which comes from the quantum numbers carried by the
 105 constituent quarks.

106 3. Results and Discussions

107 Figure 1 displays the first measurements of Ξ and Ω baryon v_1 in 10%-
 108 40% central Au+Au collisions at $\sqrt{s_{NN}} = 27$ and 200 GeV. We perform
 109 a linear fit, $v_1(y) = Cy$, where C is the fitting parameter, and y is the
 110 rapidity. We found: $C = -0.0083 \pm 0.0020$ (stat. ± 0.00 (syst.)) $[-0.0148 \pm$

Index	Quark mass	Charge	Strangeness	Δv_1 combination
1	$\Delta m = 0$	$\Delta q = 0$	$\Delta S = 0$	$[\bar{p}(\bar{u}\bar{u}\bar{d}) + \phi(s\bar{s})] - [K^-(\bar{u}s) + \bar{\Lambda}(\bar{u}\bar{d}\bar{s})]$
2	$\Delta m \approx 0$	$\Delta q = 1$	$\Delta S = 2$	$[\bar{\Lambda}(\bar{u}\bar{d}\bar{s})] - [\frac{1}{3}\Omega^-(sss) + \frac{2}{3}\bar{p}(\bar{u}\bar{u}\bar{d})]$
3	$\Delta m \approx 0$	$\Delta q = \frac{4}{3}$	$\Delta S = 2$	$[\bar{\Lambda}(\bar{u}\bar{d}\bar{s})] - [K^-(\bar{u}s) + \frac{1}{3}\bar{p}(\bar{u}\bar{u}\bar{d})]$
4	$\Delta m = 0$	$\Delta q = 2$	$\Delta S = 6$	$[\bar{\Omega}^+(\bar{s}\bar{s}\bar{s})] - [\Omega^-(sss)]$
5	$\Delta m \approx 0$	$\Delta q = \frac{7}{3}$	$\Delta S = 4$	$[\Xi^+(\bar{d}\bar{s}\bar{s})] - [K^-(\bar{u}s) + \frac{1}{3}\Omega^-(sss)]$

Table 1. Table showing difference in mass, charge, and strangeness between combinations formed from seven particle species composed of produced quarks only.

111 0.0028 (stat.) \pm 0.0013 (syst.)] for Ξ^- [Ξ^+] and $C = -0.0214 \pm 0.008$ (stat.) \pm
 112 0.0034 (syst.) [-0.0075 ± 0.0118 (stat.) \pm 0.0017 (syst.)] for Ω^- [$\bar{\Omega}^+$] at
 113 $\sqrt{s_{NN}} = 27$ GeV. There is a hint of a larger v_1 for Ω^- compared to Ξ^-
 114 baryons is observed at $\sqrt{s_{NN}} = 27$ GeV, though the uncertainties are large.

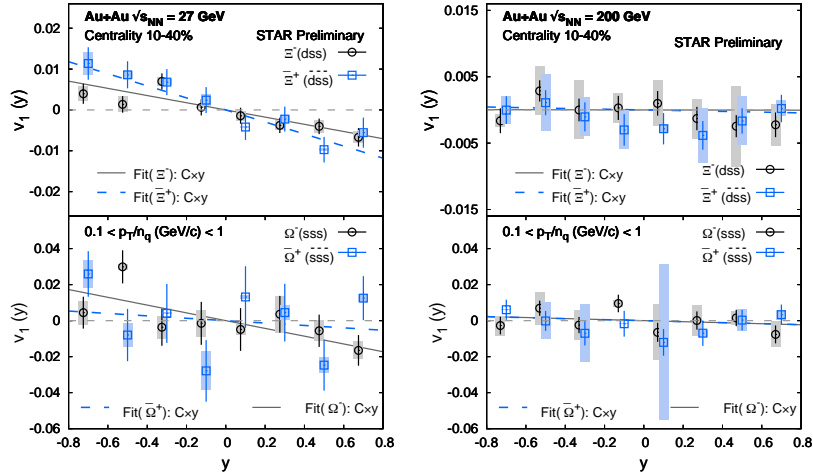


Fig. 1. v_1 of Ξ^- , Ξ^+ , Ω^- and $\bar{\Omega}^+$ as a function of rapidity, y , in 10%-40% central Au+Au collisions at $\sqrt{s_{NN}} = 27$ and 200 GeV.

115 In Fig. 2, we show the measured $\Delta v_1(y)$ for hadron combinations with
 116 $(\Delta q, \Delta S) = (0, 0), (4/3, 2)$ in 10%-40% Au+Au collisions at $\sqrt{s_{NN}} = 27$
 117 GeV. The Δv_1 -slope parameters of the measurements are extracted. For
 118 $\Delta q = 0$ and $\Delta S = 0$ (identical quark combination case), the value of the
 119 slope is a minimum compared to $\Delta q = 4/3$ and $\Delta S = 2$ cases. This minimum
 120 deviation from zero implies that the coalescence sum rule holds with the

121 identical quark combination. The deviation of the slope from zero increases
 122 as we move to $\Delta q = 4/3$ and $\Delta S = 2$ case. A Multi-Phase Transport
 123 (AMPT) [10, 11] model calculation can describe the measured Δv_1 within
 124 errors for the $\Delta q = 0$, $\Delta S = 0$ case. For $\Delta q = 4/3$ and $\Delta S = 2$, AMPT
 125 depicts a completely opposite trend compared to the data.

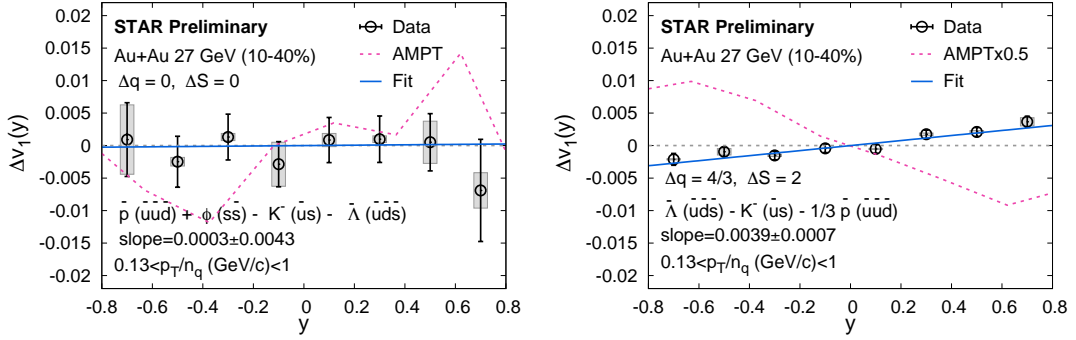


Fig. 2. Δv_1 as a function of y for $(\Delta q, \Delta S) = (0, 0), (4/3, 2)$ in Au+Au collisions at $\sqrt{s_{NN}} = 27$ GeV in 10%-40% centrality.

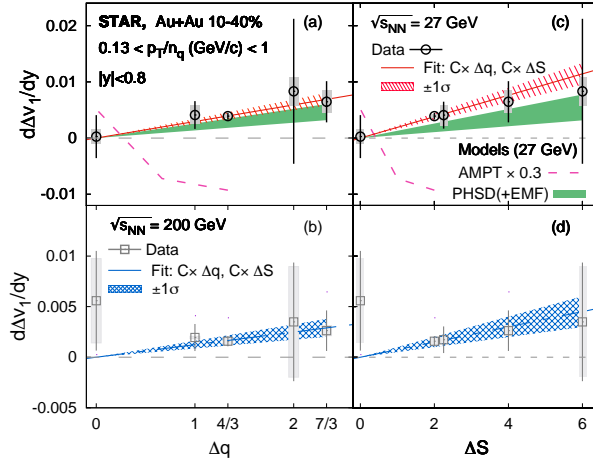


Fig. 3. Δv_1 -slope ($d\Delta v_1/dy$) as a function of Δq , and ΔS for 10%-40% centrality in Au+Au collisions at $\sqrt{s_{NN}} = 27$ GeV and $\sqrt{s_{NN}} = 200$ GeV.

126 In Fig. 3, we display the mid-rapidity Δv_1 -slope ($d\Delta v_1/dy$) as a function
 127 of Δq and ΔS for 10%-40% central Au+Au collisions at $\sqrt{s_{NN}} = 27$ and 200
 128 GeV. The $d\Delta v_1/dy$ increases with Δq and ΔS . The slope parameters of the
 129 $d\Delta v_1/dy$ with Δq , $d^2\Delta v_1/dy d\Delta q$, are $[2.952 \pm 0.489$ (stat.) ± 0.367 (syst.)] \times

130 10^{-3} and $[1.242 \pm 0.381 \text{ (stat.)} \pm 0.258 \text{ (syst.)}] \times 10^{-3}$ at $\sqrt{s_{\text{NN}}} = 27$ and 200
 131 GeV, respectively. The magnitude of the Δv_1 slope is larger at $\sqrt{s_{\text{NN}}} = 27$
 132 GeV than at 200 GeV with 4.83σ significance. The AMPT calculations [10,
 133 11] do not agree with the measurements whereas the PHSD with EM field
 134 calculations can explain the data within uncertainties. The PHSD model
 135 with EM field assumes that all electric charges are affected by the strong EM
 136 field which ensures splitting of v_1 between positive and negative particles as
 137 observed in Fig 3.

138 4. Summary

139 In summary, we present the first measurements of directed flow, $v_1(y)$,
 140 of Ξ and Ω in Au+Au collisions at $\sqrt{s_{\text{NN}}} = 27$ GeV and 200 GeV. There
 141 is a hint of a relatively larger v_1 -slope for Ω^- compared to the Ξ baryons
 142 within the uncertainties. We measure directed flow splitting, Δv_1 , with Δq
 143 and ΔS . The Δv_1 -slope for hadron combinations, increases with Δq and
 144 ΔS . The strength of the splitting increases going from $\sqrt{s_{\text{NN}}} = 200$ to 27
 145 GeV. The PHSD with EM field calculations can describe the Δq and ΔS
 146 dependent splitting within uncertainties.

147 Acknowledgments

148 Author acknowledges support from the Office of Nuclear Physics within
 149 the US DOE Office of Science, under Grant DE-FG02-89ER40531.

REFERENCES

- 150 [1] U. W. Heinz, Landolt-Bornstein, **23**, 240 (2010).
 151 [2] U. Gursoy *et al.*, *Phys. Rev. C* **89**, 054905 (2014); *Phys. Rev. C* **98**, 055201
 152 (2018).
 153 [3] STAR Collaboration, *Phys. Rev. Lett.* **118**, 012301 (2017).
 154 [4] ALICE Collaboration, *Phys. Rev. Lett.* **125**, 022301 (2020).
 155 [5] J. C. Dunlop, M. A. Lisa, and P. Sorensen, *Phys. Rev. C* **84**, 044914 (2011).
 156 [6] Y. Guo, F. Liu, and A. Tang, *Phys. Rev. C* **86**, 044901 (2012).
 157 [7] S. Gorbunov, *On-line reconstruction algorithms for the CBM and ALICE ex-*
 158 *periments*, Ph.D. thesis, Johann Wolfgang Goethe-Universitat (2013).
 159 [8] R. Barlow, in *Conference on Advanced Statistical Techniques in Particle*
 160 *Physics(2002)*, hep-ex/0207026.
 161 [9] A. I. Sheikh, D. Keane, and P. Tribedy, *Phys. Rev. C* **105**, 014912 (2022).
 162 [10] Z.-W. Lin *et al.*, *Phys. Rev. C* **72**, 064901 (2005).
 163 [11] K. Nayak, S. Shi, N. Xu, and Z.-W. Lin, *Phys. Rev. C* **100**, 054903 (2019).